

8-14-2010

## Insights into Particle Formation and Remineralization Using the Short-Lived Radionuclide, Thorium-234

Kanchan Maiti

Claudia R. Benitez-Nelson  
benitezn@mailbox.sc.edu

Ken O. Buesseler

Follow this and additional works at: [https://scholarcommons.sc.edu/geol\\_facpub](https://scholarcommons.sc.edu/geol_facpub)



Part of the [Earth Sciences Commons](#)

---

### Publication Info

Published in *Geophysical Research Letters*, Volume 37, Issue 15, 2010.

Copyright 2010 by the American Geophysical Union.

This Article is brought to you by the Earth, Ocean and Environment, School of the at Scholar Commons. It has been accepted for inclusion in Faculty Publications by an authorized administrator of Scholar Commons. For more information, please contact [dillarda@mailbox.sc.edu](mailto:dillarda@mailbox.sc.edu).

## Insights into particle formation and remineralization using the short-lived radionuclide, Thorium-234

Kanchan Maiti,<sup>1,2</sup> Claudia R. Benitez-Nelson,<sup>3</sup> and Ken O. Buesseler<sup>2</sup>

Received 20 May 2010; revised 16 June 2010; accepted 30 June 2010; published 14 August 2010.

[1] Simple mass balance models are applied to a high resolution  $^{234}\text{Th}$  profile from the northwest Pacific to examine the magnitude, rate, and depth distribution of particle remineralization processes below the euphotic zone ( $E_z$ ). Here, excess  $^{234}\text{Th}$  ( $^{234}\text{Th} > ^{238}\text{U}$ ) below the  $E_z$  is attributed to fragmentation processes that result in the conversion of sinking to non-sinking particles. By considering particulate organic carbon (POC) to  $^{234}\text{Th}$  ratios on particles, we show that POC flux attenuation is larger than for  $^{234}\text{Th}$ , which we attribute to bacterial and zooplankton consumption of sinking POC. Three case studies are used to demonstrate how different combinations of particle fragmentation and POC respiration impact flux attenuation below the  $E_z$ . When sampled with high vertical resolution and precision,  $^{234}\text{Th}$  and POC/ $^{234}\text{Th}$  ratios provide insights into both export from the  $E_z$  and the extent to which sinking particle fluxes and associated minerals are attenuated with depth. **Citation:** Maiti, K., C. R. Benitez-Nelson, and K. O. Buesseler (2010), Insights into particle formation and remineralization using the short-lived radionuclide, Thorium-234, *Geophys. Res. Lett.*, 37, L15608, doi:10.1029/2010GL044063.

### 1. Introduction

[2] Within the ocean, particle formation and dissolution plays a critical role in the cycling of many natural and anthropogenically produced elements that effect biological production, human health and even Earth's climate. One way of understanding the marine particle dynamics in the upper ocean is to utilize thorium-234 as a natural tracer of these processes.  $^{234}\text{Th}$  is a naturally occurring, short-lived radionuclide ( $t_{1/2} = 24.1$  d) produced by the radioactive decay of  $^{238}\text{U}$  ( $t_{1/2} = 4.47 \times 10^9$  y). Unlike its conservative parent,  $^{234}\text{Th}$  is highly particle reactive in seawater, making it an ideal tracer of particle dynamics within marine systems. In essence, when  $^{234}\text{Th}$  is in disequilibrium with  $^{238}\text{U}$  (total activities  $^{234}\text{Th} < ^{238}\text{U}$ ), the loss of  $^{234}\text{Th}$  on sinking particles is large relative to its production rate and rapid relative to its half life [Waples *et al.*, 2006].  $^{234}\text{Th}$  adsorbed on to sinking particles is subsequently transported into deeper waters where particle formation is reduced and remineralization processes result in non-sinking particles or conversion to dissolved phases. These remineralization processes effectively act as an

additional source of  $^{234}\text{Th}$  to subsurface waters, thereby potentially causing activities of  $^{234}\text{Th}$  in excess of that supplied by in situ  $^{238}\text{U}$  decay ( $^{234}\text{Th} > ^{238}\text{U}$ ).

[3] Most studies dealing with  $^{234}\text{Th}$  have focused on the upper ocean and the role of  $^{234}\text{Th}$  as a tracer of surface ocean particle export derived from biological activity. These studies use the ratio of carbon (or other element or compound) to  $^{234}\text{Th}$  on sinking particles to empirically convert  $^{234}\text{Th}$  derived fluxes into elements of more interest, such as particulate organic carbon (POC), biogenic silica or trace metals [e.g., Buesseler, 1998]. Although the concept of  $^{234}\text{Th}$  excess at depth is not new, many earlier studies were limited by methodology, resulting in low vertical sampling resolution [Bacon *et al.*, 1996; Usbeck *et al.*, 2002].

[4] The development of a small volume technique for  $^{234}\text{Th}$  measurements has increased both ease in sampling and precision ( $\leq 5\%$ ) [Benitez-Nelson *et al.*, 2001a, 2001b; Pike *et al.*, 2005] leading to its increasingly widespread application [Waples *et al.*, 2006]. As a result, there are now a number of high resolution vertical  $^{234}\text{Th}$  profiles where excess  $^{234}\text{Th}$  in subsurface waters is detected [Savoie *et al.*, 2004; Buesseler *et al.*, 2008; Maiti *et al.*, 2008; Buesseler *et al.*, 2009]. In many cases, excess  $^{234}\text{Th}$  activities are found immediately below the euphotic zone ( $E_z = 0.1\%$  light) and mixed layer. This excess  $^{234}\text{Th}$  peak is contained within a rather narrow layer of water where remineralization of sinking particles via fragmentation and respiration of POC by bacteria and/or zooplankton occurs at rates that are sufficient to cause a temporal excess in the subsurface  $^{234}\text{Th}$  activity (note we use remineralization to refer to the combined biological and physicochemical processes that causes particle flux attenuation).

[5] Here, we utilize a high resolution  $^{234}\text{Th}$  profile collected from the NW Pacific to examine how excess  $^{234}\text{Th}$  activities at depth, coupled with a simple mass balance model, can be used to examine the magnitude, rate, and depth distribution of particle remineralization processes below the  $E_z$ . These concepts are further expanded to the application of  $^{234}\text{Th}$  as a tracer of both surface POC export and subsequent remineralization within the twilight zone ( $E_z$  to 1000 m). The ideas presented here set the foundation for future in depth studies of  $^{234}\text{Th}$  and POC fluxes and remineralization.

### 2. Model Development and Discussion

[6] The magnitude and depth of excess  $^{234}\text{Th}$  activities are controlled by a number of different processes: the absolute flux of sinking particles (e.g., development and decline of blooms within the  $E_z$ ); the nature of the sinking particles (i.e., lability and sinking rate); subsurface remineralization (e.g., changes in zooplankton or bacterial respiration rates, and/or their depth distributions); by the physical environment (e.g.,

<sup>1</sup>Department of Oceanography and Coastal Sciences, Louisiana State University, Baton Rouge, Louisiana, USA.

<sup>2</sup>Department of Marine Chemistry and Geochemistry, Woods Hole Oceanographic Institution, Woods Hole, Massachusetts, USA.

<sup>3</sup>Department of Earth and Ocean Sciences, University of South Carolina, Columbia, South Carolina, USA.

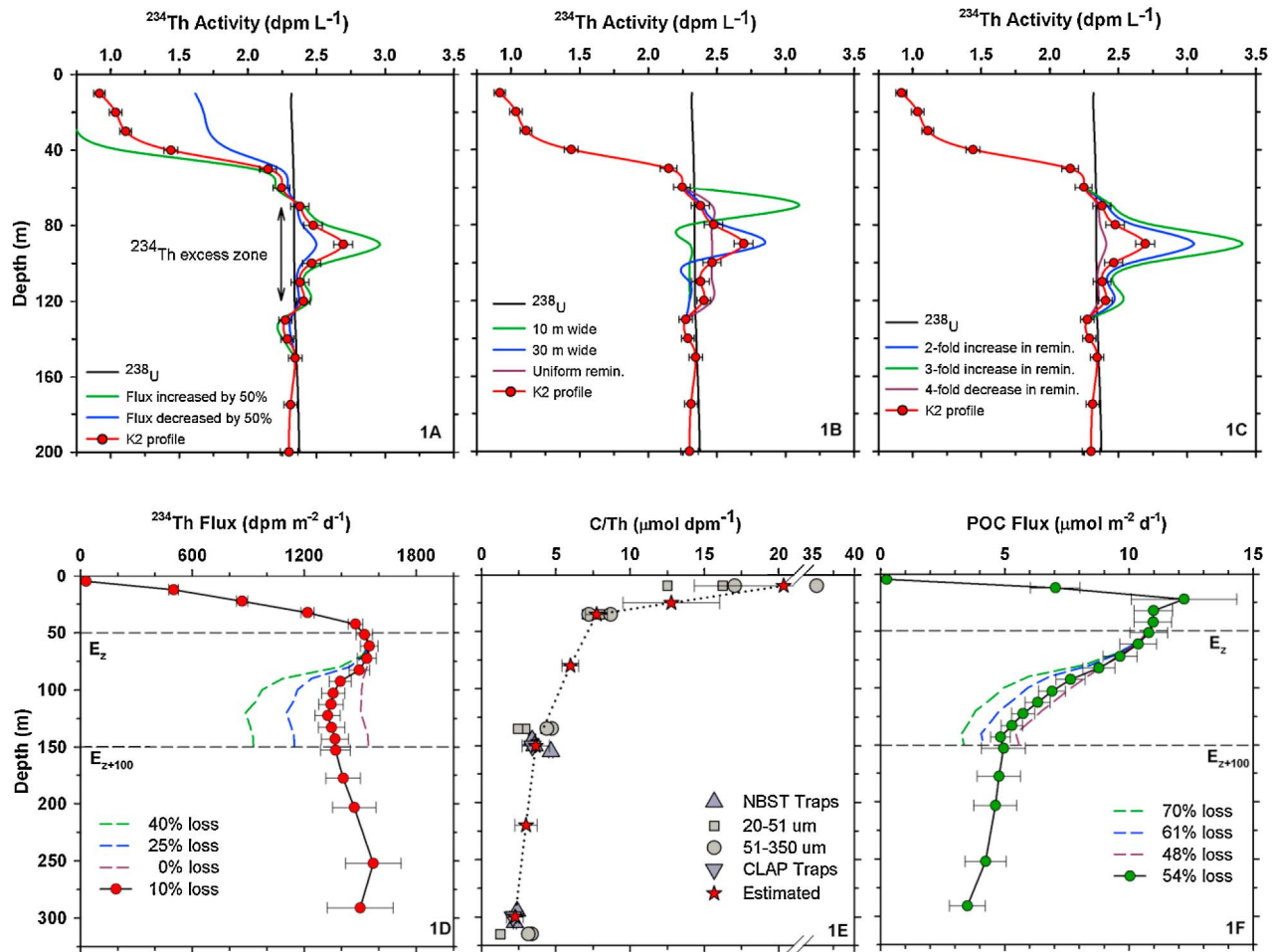


**Figure 1.** Modeled data showing how changes in (a) particle fluxes, (b) width of remineralization zone, and (c) remineralization rates affect shallow  $^{234}\text{Th}$  excess profiles. See Text S1 for model details. (d and f) The corresponding effect of change in remineralization rates (Figure 1c) on  $^{234}\text{Th}$  and POC fluxes. The dashed lines in Figure 1d represent  $^{234}\text{Th}$  and POC fluxes for the same remineralization scenarios of 2-fold increase (blue), 3-fold increase (green), and 4-fold decrease (brown) in remineralization with respect to K2 as shown in Figure 1c. (e) The C/Th ratio shown by the red stars represents the average of traps and size fractionated *in situ* pump data and is interpolated linearly between two given depths.  $^{234}\text{Th}$  profile (CTD-24) and C/Th data from Buesseler *et al.* [2009].

density discontinuities, changes to temperature or geochemistry); or some combination of the above.

[7] The models developed here (see Text S1 for details) use data from site K2 (47°N, 161°E) in the northwestern Pacific Ocean in order to illustrate a conceptual framework for interpreting the shape and size of excess  $^{234}\text{Th}$  features observed in the water column.<sup>1</sup> Using the K2  $^{234}\text{Th}$  activity profile and steady state derived  $^{234}\text{Th}$  fluxes (assuming physical processes to be negligible), we model three processes that likely influence  $^{234}\text{Th}$ :  $^{238}\text{U}$  disequilibria (both  $^{234}\text{Th}$  excess and deficiency) at any site.

## 2.1. Changes in the Flux of $^{234}\text{Th}$

[8] In order to have a significant excess of  $^{234}\text{Th}$  in the ocean, there must be a deficiency of  $^{234}\text{Th}$  somewhere else. In the open ocean, variations in the magnitude of the  $^{234}\text{Th}$  deficiency, controls the maximum extent of excess  $^{234}\text{Th}$  at

depth. This is illustrated in our K2 example by maintaining constant depth and remineralization rates while increasing or decreasing the originally measured  $^{234}\text{Th}$  export flux at 60 m by 50%. When increasing the flux by 50%, the  $^{234}\text{Th}$  deficit within the upper 60 m increases to account for the higher  $^{234}\text{Th}$  flux (green line Figure 1a). Using a higher flux but the same remineralization rates between 60–120 m, results in greater excess  $^{234}\text{Th}$ . The reverse is true when the flux is decreased by 50% (blue line Figure 1a), resulting in a less prominent  $^{234}\text{Th}$  excess zone that can be easily missed by low resolution  $^{234}\text{Th}$  profiles.

## 2.2. Width of Remineralization Zone

[9] In the K2 profile, the most prominent zone of remineralization is just below the  $E_z$  between 60 and 120 m, where  $\sim 220 \text{ dpm m}^{-2} \text{ d}^{-1}$  of the  $^{234}\text{Th}$  flux is remineralized. However, the relative contribution of the different depth horizons to the total  $^{234}\text{Th}$  remineralized is not uniform. If the same amount of  $^{234}\text{Th}$  remineralization were to take place with uniform intensity between 60–120 m, it would result in a

<sup>1</sup>Auxiliary materials are available in the HTML. doi:10.1029/2010GL044063.

plateau of  $^{234}\text{Th}$  excess (Figure 1b, brown line) and this is not observed. On the other hand, if remineralization was limited to within a 10 m (i.e. between 60–70 m) or a 30 m (i.e. between 60–90 m) wide layer, the peak in  $^{234}\text{Th}$  excess becomes more intense and clearly identifiable (Figure 1b). Unfortunately, these narrow peaks also become relatively easier to miss without high resolution sampling, since they are essentially defined by only one or two  $^{234}\text{Th}$  data points.

### 2.3. Variable Rates of Remineralization

[10] In order to understand the sensitivity of the  $^{234}\text{Th}$  profiles to changes in remineralization rates between 60 and 120 m, the fraction of  $^{234}\text{Th}$  remineralized in this zone is increased by 2–3 fold or decreased by 4 fold from that observed in the original data (Figure 1c, red line). When the remineralization rate increases, the  $^{234}\text{Th}$  excess peak becomes increasingly prominent and is more easily identified (Figure 1c). In contrast, when the remineralization rate is decreased, it becomes more difficult to identify any  $^{234}\text{Th}$  excess in the profile. In the current example (Figure 1c, brown line) even with samples collected at 10 m sampling intervals, it would be difficult to detect excess  $^{234}\text{Th}$  if the remineralization rate decreased by more than two fold since the  $^{234}\text{Th}$  activities in the remineralization zone become indistinguishable from  $^{238}\text{U}$  beyond analytical uncertainty (Figure 1c).

[11] Using the model calculations, we demonstrate how simple changes in  $^{234}\text{Th}$  flux, the depth over which that remineralization occurs, and remineralization rate, influences the magnitude and location of excess  $^{234}\text{Th}$  within the water column. In the ocean, the manifestation of excess  $^{234}\text{Th}$  in the water column is likely controlled by multiple processes. For example, the absence of a clear  $^{234}\text{Th}$  excess layer even within a high resolution profile does not necessarily mean that there is no significant remineralization. Rather, it could simply be spread out over a wider depth zone that does not allow for clear identification of a  $^{234}\text{Th}$  excess peak within analytical uncertainties (similar to brown line in Figure 1b). What can be said, however, is that if an excess  $^{234}\text{Th}$  peak is observed, it generally indicates a rather narrow layer of more intense remineralization (10's of meters) that is larger than 10% of the overlying  $^{234}\text{Th}$  particle flux. For any given profile, the models described here allow one to set limits on the extent of  $^{234}\text{Th}$  remineralization and depth over which these higher remineralization rates occur.

### 3. $^{234}\text{Th}$ as a Proxy for POC Remineralization

[12] In this section, we combine the  $^{234}\text{Th}$  flux and remineralization models with  $\text{POC}/^{234}\text{Th}$  data, to examine POC flux attenuation, focusing on the 100 m layer immediately below the  $E_z$  ( $E_{z+100}$ ). It is within this layer that regional and temporal differences in POC flux attenuation are typically largest [Buesseler and Boyd, 2009]. Using the K2 example,  $^{234}\text{Th}$  fluxes would reach a maximum around 60 m, and then decrease such that the net  $^{234}\text{Th}$  flux at  $E_{z+100}$  is about 10% lower than at  $E_z$  (Figure 1d). As a sensitivity analysis, we also plotted a wider range of possible  $^{234}\text{Th}$  remineralization scenarios (as shown in Figure 1c) where the loss in  $^{234}\text{Th}$  flux between  $E_z$  and  $E_{z+100}$  varies between 0 and 40% (Figure 1d). For example, when the remineralization rate increases by three fold (Figure 1c, green line) or two fold (Figure 1c, blue line) or decreases by four fold (Figure 1c, brown line), there is a corresponding decrease in  $^{234}\text{Th}$  flux at

$E_{z+100}$  by 40% (Figure 1d, green line), 25% (Figure 1d, blue line) and 0% (Figure 1d, brown line) respectively.

[13] The  $\text{POC}/^{234}\text{Th}$  ratio at K2 (hereafter abbreviated as C/Th) decreases from  $>15\text{--}20 \mu\text{M dpm}^{-1}$  to  $<3\text{--}5 \mu\text{mol dpm}^{-1}$  below 100 m (Figure 1e). As in other studies, variability in C/Th is greatest in the  $E_z$  and decreases with depth (see review by Buesseler *et al.* [2006]). Here C/Th is the same in both sediment traps and on the larger particle size classes collected on 20 and 51  $\mu\text{m}$  nominal pore size screens. We calculate the POC flux by multiplying the  $^{234}\text{Th}$  flux by a straight line fit to the C/Th data (Figure 1f). The decrease in  $^{234}\text{Th}$  and POC flux from  $E_z$  to  $E_{z+100}$  is 10% and 54% respectively for the K2 profile. However for the same changes in remineralization rate as shown in Figure 1c, the  $^{234}\text{Th}$  flux decreases by 0–40% where as the POC flux decreases from 48–70% between  $E_z$  and  $E_{z+100}$  (Figures 1d and 1f). Interestingly in these two figures, the flux attenuation between  $E_z$  and  $E_{z+100}$  is much larger for POC (48–70%) than for  $^{234}\text{Th}$  (0–40%) due to the decrease in C/Th with depth (Figure 1e). However it must be noted that changes in remineralization rate may also affect the C/Th which is not taken into account in our model formulation.

[14] Conceptually, we hypothesize that differences in the  $^{234}\text{Th}$  and POC flux profiles provide important insights into the processes that control flux attenuation. The  $^{234}\text{Th}$  excess at depth can be attributed to any process that results in the conversion of sinking to non-sinking particles, to which  $^{234}\text{Th}$  is attached. We will call this process fragmentation, as fragmentation of fecal pellets or marine snow by zooplankton (coprohexy) is a common example of this type of process [Lampitt *et al.*, 1990]. However, other processes such as particle disaggregation due to physical-chemical processes, or even a decrease in particle sinking speed to the point where the flux per day is slower than the ingrowth and decay of  $^{234}\text{Th}$ , would all decrease the  $^{234}\text{Th}$  flux. Sinking POC on the other hand, is a food source for mesopelagic bacteria and zooplankton. Thus, in addition to fragmentation processes, POC flux will be attenuated due to respiration within the mesopelagic. This second process would not necessarily alter the flux of  $^{234}\text{Th}$  (though it may indirectly by changing particle properties). In this example, fragmentation processes decrease both  $^{234}\text{Th}$  and POC fluxes by 10%, while the POC flux will be further attenuated by an additional 44% due to C respiration processes (0 to 10% change due to fragmentation for  $^{234}\text{Th}$ , and 44% to 54% for POC due to respiration). Please note that the possible loss of POC via formation of dissolved organic carbon is not taken into consideration in this paper.

[15] In the following section, we examine three other settings where the vertical  $^{234}\text{Th}$  and C/Th resolution is not as high, but still sufficient to illustrate regional and temporal variability in flux attenuation. These studies help to illustrate the relative importance of C respiration and particle fragmentation processes in controlling overall particle flux remineralization in the open ocean.

## 4. $^{234}\text{Th}$ Derived Particle Remineralization: Comparison of Three Study Sites

### 4.1. Case 1

[16] In a study of the impact of mesoscale eddies on upper ocean biogeochemistry in the Sargasso Sea [McGillicuddy *et al.*, 2007], an excess  $^{234}\text{Th}$  peak was observed at all stations, but especially at the center of a cyclonic eddy, where

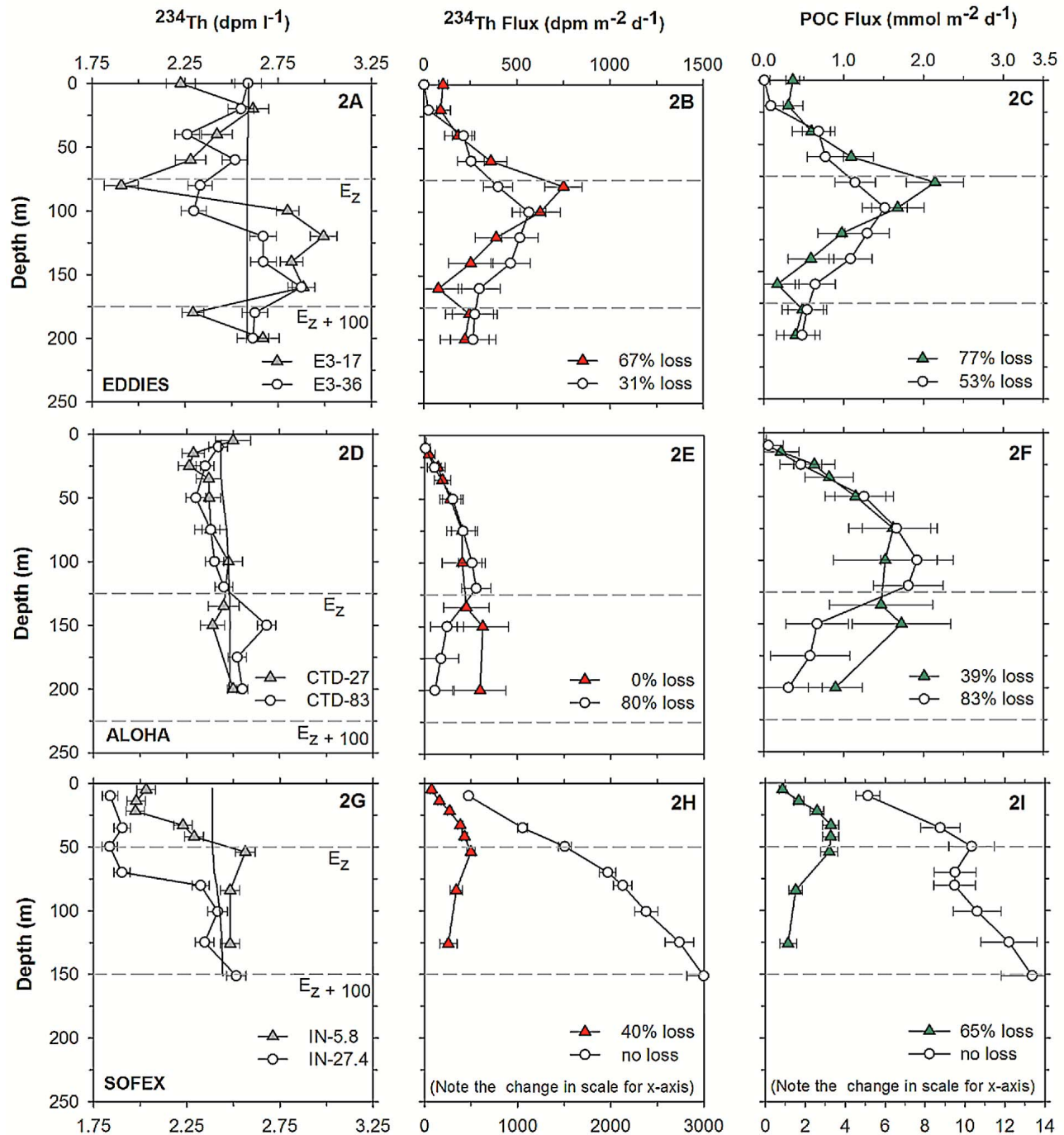


**Figure 2.** Examples from the three case study areas showing profiles of  $^{234}\text{Th}$  activity,  $^{234}\text{Th}$  flux, and POC flux. The C/Th data (not shown) and the station IDs are the same as that in the referred papers (see text for details).

prominent excess  $^{234}\text{Th}$  peaks were found immediately below the euphotic zone [Buesseler *et al.*, 2008]. The excess  $^{234}\text{Th}$  activities between the base of the  $E_z$  and  $E_z+100$  (Figure 2a) leads to decreases in the  $^{234}\text{Th}$  flux by 67 and 31% (Figure 2b) and even larger decreases in POC flux, by 77 and 53% (Figure 2c) as C/Th decreases as well. At K2 a 10% decrease in  $^{234}\text{Th}$  flux resulted in a 54% decrease in POC flux. The reduced sensitivity of  $^{234}\text{Th}$  flux to changes in the POC flux within these eddies suggests that fragmentation processes, as evidenced by higher  $^{234}\text{Th}$  flux losses), are more dominant than respiration in comparison to the K2 site. The

greater POC loss due to respiration at K2 is supported by upper 150 m water column data which indicate much higher zooplankton and bacterial production at K2 (zooplankton biomass  $\approx 3500 \text{ mg m}^{-2}$  [Steinberg *et al.*, 2008]; BP  $\approx 62 \text{ mg C m}^{-2} \text{ d}^{-1}$  [Boyd *et al.*, 2008]) relative to inside the eddies (zooplankton biomass  $\approx 700 \text{ mg m}^{-2}$  [Goldthwait and Steinberg, 2008]; BP  $\approx 17 \text{ mg C m}^{-2} \text{ d}^{-1}$  [Ewart *et al.*, 2008]).

#### 4.2. Case 2

[17] Station ALOHA in the subtropical Pacific Ocean, is characterized by very low  $^{234}\text{Th}$  disequilibria, resulting in

$^{234}\text{Th}$  fluxes averaging only  $400 \pm 400 \text{ dpm m}^{-2} \text{ d}^{-1}$  at the base of the  $E_z$  [Buesseler et al., 2009]. The system is characterized by small picoplankton and grazers, with a deep chlorophyll maxima and extensive recycling of POC in the upper 125 m leading to low export ratios of 7% [Buesseler and Boyd, 2009]. A few of these profiles show a slight  $^{234}\text{Th}$  excess below the  $E_z$  (Figure 2d) and illustrate our earlier model discussions that with low surface  $^{234}\text{Th}$  fluxes, excess  $^{234}\text{Th}$  peaks are very difficult to discern (blue line in Figure 1a). In the first profile (solid triangle in Figure 2e) there is 0% loss in  $^{234}\text{Th}$  flux between  $E_z$  and  $E_{z+100}$  with a corresponding 39% loss in POC flux (solid triangle in Figure 2f). This suggests a dominant role of respiration over fragmentation. However the other profile (solid circle in Figures 2e and 2f) collected 10 days later shows very similar loss in both  $^{234}\text{Th}$  flux (80%) and POC (83%) indicating a shift towards fragmentation. Sufficient biological data was not collected during these two profiles to understand what caused the shift in the fragmentation and respiration processes. The presence of a detectable  $^{234}\text{Th}$  excess peak in this profile and from both the profiles from Sargasso eddies may suggest that prominent  $^{234}\text{Th}$  excess peaks are more often associated with fragmentation processes.

### 4.3. Case 3

[18] During this iron enrichment experiment, biological production was enhanced in HNLC waters south of the Polar Front [Buesseler et al., 2004]. The  $^{234}\text{Th}$  profiles shown here are from days 6 and 27 during which they changed significantly, showing a large decrease in total  $^{234}\text{Th}$  in the upper 70 m and elimination of the  $^{234}\text{Th}$  excess below the  $E_z$  (Figure 2g). The result is an increase in overall export flux from the  $E_z$  for both  $^{234}\text{Th}$  and POC (Figures 2h and 2i). Of importance to this discussion is the narrow layer of significant POC flux attenuation below the  $E_z$  early in the bloom where  $^{234}\text{Th}$  flux and POC flux decreases by 40 and 65% respectively between  $E_z$  and  $E_{z+100}$  (solid triangles in Figures 2h and 2i). During this stage both fragmentation and respiration played an important role in remineralization. However, later in the experiment there is an increase in the POC export below the  $E_z$  resulting in no net loss of  $^{234}\text{Th}$  or POC between  $E_z$  and  $E_{z+100}$  (circles in Figures 2h and 2i). The changes below  $E_z$  suggests either more efficient transport of sinking POC due to differences in sinking particle properties (such as sinking rate, particle lability), and/or a change in remineralization possibly due to shift in the depth of maximal zooplankton feeding [Buesseler et al., 2005]. This may have resulted in very little fragmentation and lower respiration in this zone leading to negligible attenuation of  $^{234}\text{Th}$  and POC flux. Biological data were not collected with sufficient resolution to resolve the causes, but this is another example of where  $^{234}\text{Th}$  was able to document not only a change in POC export from the  $E_z$ , but a very dynamic shift in POC attenuation below the  $E_z$  over a span of three weeks.

## 5. Summary and Future Work

[19] Throughout the water column, attached and free living bacteria recycle organic matter, breaking down POC into colloidal and dissolved organic and inorganic forms of C, thereby changing particle properties and stickiness (e.g. TEP) [Passow et al., 2001]. Thus, bacteria can potentially increase, or more generally, decrease POC fluxes [Taylor et al., 2001;

Azam et al., 1992]. Zooplankton grazing can create or aggregate particles during feeding, resulting in the production of rapidly sinking fecal material, and/or fragment sinking particles by their feeding activities. As they consume POC they produce dissolved organic matter (DOM) and respire some C as dissolved inorganic C. Zooplankton can also actively transport DOM and POC from the surface to depth by vertical migration, though this is highly variable [Longhurst et al., 1990; Wilson et al., 2008].

[20]  $^{234}\text{Th}$  provides a novel mechanism by which the above processes may be further examined and understood, by pinpointing the depths and extent to which the flux of sinking particles and associated minerals are attenuated. This is clearly evident in the K2 example and case studies, where layers immediately below the  $E_z$  contain sufficient rates of remineralization to result in POC flux attenuations even when  $^{234}\text{Th}$  flux sometimes remain relatively unchanged. Such knowledge can only be gained through high resolution vertical studies, and this is a major advantage of  $^{234}\text{Th}$  over other methods like sediment traps. Ultimately, we would like to use this approach to better constrain the bacterial and zooplankton processes responsible for the fragmentation and respiration of sinking particles as they sink through the water column. This will require not only high resolution sampling of  $^{234}\text{Th}$  activities, but also the C/Th activity on sinking particles. Furthermore, biological community structure and activity need to be sampled at similar resolution. In this manner, it will be possible to not only examine particle remineralization processes relative to  $^{234}\text{Th}$  and C, but other biologically relevant elements, such as nitrogen, phosphorus, biogenic silica, and trace metals.

[21] **Acknowledgments.** The data presented here are from a number of studies funded by the National Science Foundation. Special thanks to Steve Pike for collection and analyses of many of the  $^{234}\text{Th}$  samples.

## References

- Azam, F., et al. (1992), Bacterial transformation and transport of organic matter in the Southern California Bight, *Prog. Oceanogr.*, 30(1–4), 151–166, doi:10.1016/0079-6611(92)90011-N.
- Bacon, M. P., et al. (1996), Export flux of carbon at the equator during the EqPac time-series cruises estimated from  $^{234}\text{Th}$  measurements, *Deep Sea Res., Part II*, 43(4–6), 1133–1153, doi:10.1016/0967-0645(96)00016-1.
- Benitez-Nelson, C. R., et al. (2001a), Testing a new small-volume technique for determining thorium-234 in seawater, *J. Radioanal. Nucl. Chem.*, 248(3), 795–799, doi:10.1023/A:1010621618652.
- Benitez-Nelson, C., K. O. Buesseler, D. M. Karl, and J. Andrews (2001b), A time-series study of particulate matter export in the North Pacific Subtropical Gyre based on  $^{234}\text{Th}$ : $^{238}\text{U}$  disequilibrium, *Deep Sea Res., Part I*, 48(12), 2595–2611, doi:10.1016/S0967-0637(01)00032-2.
- Boyd, P. W., et al. (2008), Quantifying the surface-subsurface biogeochemical coupling during the VERTIGO ALOHA and K2 studies, *Deep Sea Res., Part II*, 55(14–15), 1578–1593, doi:10.1016/j.dsr2.2008.04.010.
- Buesseler, K. O. (1998), The decoupling of production and particulate export in the surface ocean, *Global Biogeochem. Cycles*, 12(2), 297–310, doi:10.1029/97GB03366.
- Buesseler, K. O., and P. W. Boyd (2009), Shedding light on processes that control particle export and flux attenuation in the twilight zone of the open ocean, *Limnol. Oceanogr.*, 54, 1210–1232.
- Buesseler, K. O., et al. (2004), The effects of iron fertilization on carbon sequestration in the Southern Ocean, *Science*, 304(5669), 414–417, doi:10.1126/science.1086895.
- Buesseler, K. O., et al. (2005), Particle export during the Southern Ocean Iron Experiment (SOFEX), *Limnol. Oceanogr.*, 50, 311–327, doi:10.4319/lo.2005.50.1.0311.
- Buesseler, K. O., et al. (2006), An assessment of particulate organic carbon to thorium-234 ratios in the ocean and their impact on the application of  $^{234}\text{Th}$  as a POC flux proxy, *Mar. Chem.*, 100(3–4), 213–233, doi:10.1016/j.marchem.2005.10.013.

- Buesseler, K. O., et al. (2008), Particle fluxes associated with mesoscale eddies in the Sargasso Sea, *Deep Sea Res., Part II*, 55(10–13), 1426–1444, doi:10.1016/j.dsr2.2008.02.007.
- Buesseler, K. O., et al. (2009), Thorium-234 as a tracer of spatial, temporal and vertical variability in particle flux in the North Pacific, *Deep Sea Res., Part I*, 56(7), 1143–1167, doi:10.1016/j.dsr.2009.04.001.
- Ewart, C. S., et al. (2008), Microbial dynamics in cyclonic and anticyclonic mode-water eddies in the northwestern Sargasso Sea, *Deep Sea Res., Part II*, 55(10–13), 1334–1347, doi:10.1016/j.dsr2.2008.02.013.
- Goldthwait, S. A., and D. K. Steinberg (2008), Elevated biomass of mesozooplankton and enhanced fecal pellet flux in cyclonic and mode-water eddies in the Sargasso Sea, *Deep Sea Res., Part II*, 55(10–13), 1360–1377, doi:10.1016/j.dsr2.2008.01.003.
- Lampitt, R. S., et al. (1990), What happens to zooplankton faecal pellets? Implications for material flux, *Mar. Biol. Berlin*, 104, 15–23, doi:10.1007/BF01313152.
- Landry, M. R., et al. (2008), Mesozooplankton biomass and grazing responses to Cyclone Opal, a subtropical mesoscale eddy, *Deep Sea Res., Part II*, 55(10–13), 1378–1388, doi:10.1016/j.dsr2.2008.01.005.
- Longhurst, A. R., et al. (1990), Vertical flux of respiratory carbon by oceanic diel migrant biota, *Deep Sea Res., Part A*, 37(4), 685–694, doi:10.1016/0198-0149(90)90098-G.
- Maiti, K., et al. (2008), The influence of a mature cyclonic eddy on particle export in the lee of Hawaii, *Deep Sea Res., Part II*, 55(10–13), 1445–1460, doi:10.1016/j.dsr2.2008.02.008.
- McGillicuddy, D. J., Jr., (2007), Eddy/wind interactions stimulate extraordinary mid-ocean plankton blooms, *Science*, 316(5827), 1021–1026, doi:10.1126/science.1136256.
- Passow, U., et al. (2001), The origin of transparent exopolymer particles (TEP) and their role in the sedimentation of particulate matter, *Cont. Shelf Res.*, 21(4), 327–346, doi:10.1016/S0278-4343(00)00101-1.
- Pike, S. M., et al. (2005), Quantification of <sup>234</sup>Th recovery in small volume sea water samples by inductively coupled plasma-mass spectrometry, *J. Radioanal. Nucl. Chem.*, 263(2), 355–360.
- Savoie, N., et al. (2004), <sup>234</sup>Th deficit and excess in the Southern Ocean during spring 2001: Particle export and remineralization, *Geophys. Res. Lett.*, 31, L12301, doi:10.1029/2004GL019744.
- Steinberg, D. K., et al. (2008), A comparison of mesopelagic mesozooplankton community structure in the subtropical and subarctic North Pacific Ocean, *Deep Sea Res., Part II*, 55(14–15), 1615–1635, doi:10.1016/j.dsr2.2008.04.025.
- Taylor, G. T., et al. (2001), Chemoautotrophy in the redox transition zone of the Cariaco Basin: A significant midwater source of organic carbon production, *Limnol. Oceanogr.*, 46, 148–163, doi:10.4319/lo.2001.46.1.0148.
- Usbeck, R., et al. (2002), Shallow remineralization in the Weddell Gyre, *Geochem. Geophys. Geosyst.*, 3(1), 1008, doi:10.1029/2001GC000182.
- Waples, J. T., et al. (2006), An introduction to the application and future use of <sup>234</sup>Th in aquatic systems, *Mar. Chem.*, 100(3–4), 166–189, doi:10.1016/j.marchem.2005.10.011.
- Wilson, S. E., et al. (2008), Changes in fecal pellet characteristics with depth as indicators of zooplankton repackaging of particles in the mesopelagic zone of the subtropical and subarctic North Pacific Ocean, *Deep Sea Res., Part II*, 55(14–15), doi:10.1016/j.dsr2.2008.04.019.

C. R. Benitez-Nelson, Department of Earth and Ocean Sciences, University of South Carolina, Columbia, SC 29201, USA.

K. O. Buesseler, Department of Marine Chemistry and Geochemistry, Woods Hole Oceanographic Institution, Woods Hole, MA 02543, USA.

K. Maiti, Department of Oceanography and Coastal Sciences, Louisiana State University, Baton Rouge, LA 70808, USA.